Linear Power-Flow Models in Multiphase Distribution Networks

Preprint

Andrey Bernstein and Emiliano Dall'Anese
National Renewable Energy Laboratory

Presented at the 7th IEEE International Conference on Innovative Smart Grid Technologies (ISGT Europe 2017)
Torino, Italy
September 26–29, 2017

NREL is a national laboratory of the U.S. Department of Energy
Office of Energy Efficiency & Renewable Energy
Operated by the Alliance for Sustainable Energy, LLC

This report is available at no cost from the National Renewable Energy Laboratory (NREL) at www.nrel.gov/publications.

Conference Paper
NREL/CP-5D00-68139
May 2017

Contract No. DE-AC36-08GO28308

NOTICE

This report is available at no cost from the National Renewable Energy Laboratory (NREL) at www.nrel.gov/publications.

Available electronically at SciTech Connect http:/www.osti.gov/scitech

Available for a processing fee to U.S. Department of Energy and its contractors, in paper, from:

U.S. Department of Energy
Office of Scientific and Technical Information
P.O. Box 62
Oak Ridge, TN 37831-0062
OSTI http://www.osti.gov
Phone: 865.576.8401
Fax: 865.576.5728
Email: reports@osti.gov

Available for sale to the public, in paper, from:

U.S. Department of Commerce
National Technical Information Service
5301 Shawnee Road
Alexandria, VA 22312
NTIS http://www.ntis.gov
Phone: 800.553.6847 or 703.605.6000
Fax: 703.605.6900
Email: orders@ntis.gov

Cover Photos by Dennis Schroeder: (left to right) NREL 26173, NREL 18302, NREL 19758, NREL 29642, NREL 19795.

NREL prints on paper that contains recycled content.

Linear Power-Flow Models in Multiphase Distribution Networks

Andrey Bernstein and Emiliano Dall'Anese

***Abstract*—This paper considers multiphase unbalanced distribution systems and develops approximate AC power-flow models wherein voltages, line currents, and powers at the point of common coupling are linearly related to the nodal net power injections. The linearization approach is grounded on a fixed-point interpretation of the AC power-flow equations, and it is applicable to distribution systems featuring a variety of connections for loads and generation units (e.g., wye and ungrounded delta, as well as line-to-line and line-to-grounded-neutral at the secondary of the distribution transformers). The approximate linear models can be naturally leveraged to facilitate the development of computationally-affordable optimization and control applications — from applications for advanced distribution management systems to online and distributed optimization routines. The approximation accuracy of the proposed method is evaluated on different feeders.**

I. Introduction

Nonlinearity of the AC power-flow equations poses significant challenges for the development of computationally-affordable control and optimization tasks – with applications ranging from traditional centralized state-estimation and dispatch problems [1]–[3] to emerging real-time distributed optimization frameworks [4], [5]. For example, the nonlinearity of the (exact) AC power-flow equations renders difficult the centralized and distributed solution of AC optimal power flow (OPF) problems; recent approaches involve convex relaxation methods (e.g., semidefinite program [1]) and linearization techniques [6]–[8]. Approximate linear models have been recently utilized to facilitate the development of real-time and distributed OPF solvers for distribution systems [4], [5] with optimality and input-to-state stability guarantees. Similarly, approximate linear models have been leveraged to design decentralized control algorithms under the purview of well-defined stability criteria [9], [10].

This paper focuses on the so-called fixed-point linearization method recently proposed in [11]. The linear approximation methodology is applicable to multiphase distribution networks with generic topologies (either radial or meshed) and multiphase constant-power buses [12]. At each multiphase node, the model of the distribution system can have: (i) grounded wye-connected loads/sources; (ii) ungrounded delta connections; (iii) a combination of wye-connected and delta-connected loads/sources; or, (iv) a combination of line-to-line and line-to-grounded-neutral devices at the secondary of the distribution transformers [12]. Models (i)–(iii) pertain to settings when the network model is limited to (aggregate) nodal power injections at the primary side of the distribution transformers. Particularly, the combined model (iii) can be utilized when different distribution transformers with either delta and/or wye primary connections are bundled together at one bus for network reduction purposes (e.g., when two transformers are connected through a short, low-impedance distribution line); see Figure 1(a) for an illustration. Load model (iv) is common, for example, in North America for commercial buildings and residential customers, and it can be utilized when the network model includes the secondary side of the distribution transformers; see Figure 1(b) and test feeders [13], [14]. Settings with only line-to-line or line-to-ground connections at the secondary are subsumed by model (iv).

Expanding on [11], we derive linear models for the (i) voltage phasors, (ii) voltage magnitudes, (iii) line currents, and (iv) power flows at the substation. We show numerically that these models provide a very good approximation to the exact power-flow solution over a wide range of loading conditions and network scale. The proposed linear models have several important advantages. First, they are computationally more affordable compared to, e.g., the first-order Taylor method [6]. Second, we show that the coefficients of the models can be updated in a distributed fashion. We illustrate this property by designing network-cognizant droop controllers. Finally, they provide a better global approximation than classical local methods.

The methodology proposed in the present paper can be utilized to broaden the applicability of [3]–[5], [10] to multiphase unbalanced distribution systems.

Notation: Upper-case (lower-case) boldface letters are used for matrices (column vectors); $(\cdot)^{\mathsf{T}}$ for transposition; $|\cdot|$ for the absolute value of a number or the element-wise absolute value of a vector or a matrix; and the letter $\jmath$ for $\jmath := \sqrt{-1}$. For a complex number $c \in \mathbb{C}$, $\Re\{c\}$ and $\Im\{c\}$ denote its real and imaginary part, respectively; and $\bar{c}$ denotes the conjugate of c. For a given $N \times 1$ vector $\mathbf{x} \in \mathbb{C}^N$, $\|\mathbf{x}\|_\infty := \max(|x_1|...|x_n|)$, $\|\mathbf{x}\|_1 := \sum_{i=1}^N |x_i|$, and $\mathbf{diag}(\mathbf{x})$ returns a $N \times N$ matrix with the elements of $\mathbf{x}$ in its diagonal. For an $M \times N$ matrix $\mathbf{A} \in \mathbb{C}^{M \times N}$, the ℓ_∞-induced norm is defined as $||\mathbf{A}||_\infty = \max_{i=1,...,M} \sum_{j=1}^N |\mathbf{A}_{ij}|$. Finally, for a vector-

Authors are with the National Renewable Energy Laboratory, Golden, CO. E-mail: {andrey.bernstein, emiliano.dallanese}@nrel.gov.

This work was supported by the U.S. Department of Energy under Contract No. DE-AC36-08GO28308 with the National Renewable Energy Laboratory. Funding provided by the Advanced Research Projects Agency-Energy (ARPA-E) under the Network Optimized Distributed Energy Systems (NODES) program. The U.S. Government retains and the publisher, by accepting the article for publication, acknowledges that the U.S. Government retains a nonexclusive, paid-up, irrevocable, worldwide license to publish or reproduce the published form of this work, or allow others to do so, for U.S. Government purposes.

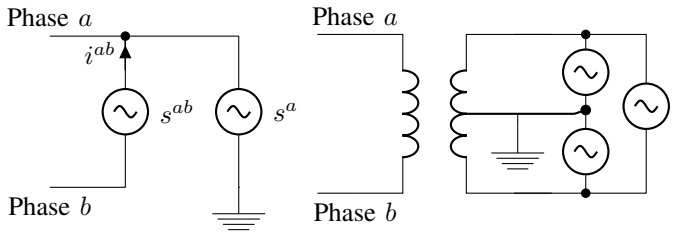

(a) (b)

Fig. 1: Examples of a multiphase point of connection (for simplicity, only two phases are shown): (a) combination of wye-connected and delta-connected loads/sources at the primary of the feeder (e.g., because of network reduction procedures); (b) combination of line-to-line loads/sources and line-to-grounded-neutral devices at the secondary of the distribution transformer.

valued map $\mathbf{x} : \mathbf{y} \in \mathbb{R}^{N\times 1} \to \mathbf{x}(\mathbf{y}) \in \mathbb{C}^{M\times 1}$, we let $\partial\mathbf{x}/\partial\mathbf{y}$ denote the $M \times N$ complex matrix with elements $(\partial\mathbf{x}/\partial\mathbf{y})_{ik} = \partial\mathbf{x}_i/\partial\mathbf{y}_k = \partial\Re\{\mathbf{x}_i\}/\partial\mathbf{y}_k + \jmath\partial\Im\{\mathbf{x}_i\}/\partial\mathbf{y}_k$, $i = 1,\dots,M$, $k = 1,\dots,N$.

II. Problem Formulation

For brevity, the problem is outlined for three-phase systems; we describe in Remark 1 below how to apply the analysis to the general multiphase case (as we do in the numerical examples in Section IV). Consider a generic three-phase distribution network with one slack bus and N PQ buses. With reference to the example illustrated in Figure 1, let $\mathbf{s}_j^Y := (s_j^a, s_j^b, s_j^c)^\mathsf{T}$ denote the vector of the grounded wye sources at node j, where $s_j^\phi \in \mathbb{C}$ denotes the net complex power injected on phase ϕ. Similarly, let $\mathbf{s}_j^\Delta := (s_j^{ab}, s_j^{bc}, s_j^{ca})^\mathsf{T}$ denote the power injections of the delta-connected sources. With a slight abuse of notation, $\mathbf{s}_j^Y$ and $\mathbf{s}_j^\Delta$ represent line-to-line connections and line-to-ground connections, respectively, when bus j corresponds to the secondary side of the distribution transformer (this notational choice allows us to avoid additional symbols).

At bus j, the following set of equations relates voltages, currents, and power injections:

$$\begin{cases} s_j^{ab} = (v_j^a - v_j^b)\overline{i_j^{ab}}, \\ s_j^{bc} = (v_j^b - v_j^c)\overline{i_j^{bc}}, \\ s_j^{ca} = (v_j^c - v_j^a)\overline{i_j^{ca}}, \\ v_j^a(\overline{i_j^{ab}} - \overline{i_j^{ca}}) + s_j^a = v_j^a\overline{i_j^a}, \\ v_j^b(\overline{i_j^{bc}} - \overline{i_j^{ab}}) + s_j^b = v_j^b\overline{i_j^b}, \\ v_j^c(\overline{i_j^{ca}} - \overline{i_j^{bc}}) + s_j^c = v_j^c\overline{i_j^c}, \end{cases}$$

where $\mathbf{v}_j = (v_j^a, v_j^b, v_j^c)^\mathsf{T}$, $\mathbf{i}_j = (i_j^a, i_j^b, i_j^c)^\mathsf{T}$, and $\mathbf{i}_j^\Delta = (i_j^{ab}, i_j^{bc}, i_j^{ca})^\mathsf{T}$ collect the phase-to-ground voltages $\{v_j^\phi\}_{\phi\in\{a,b,c\}}$, phase net current injections $\{i_j^\phi\}_{\phi\in\{a,b,c\}}$, and phase-to-phase currents $\{i_j^{\phi\phi'}\}_{\phi,\phi'\in\{a,b,c\}}$ (for the delta connections and line-to-line connections) of node j, respectively.

We next express the set of power-flow equations in vector-matrix form. To that end, let $\mathbf{v}_0 := (v_0^a, v_0^b, v_0^c)^\mathsf{T}$, $\mathbf{i}_0 := (i_0^a, i_0^b, i_0^c)^\mathsf{T}$, and $\mathbf{s}_0 := (s_0^a, s_0^b, s_0^c)^\mathsf{T}$ denote the complex vectors collecting the three-phase nodal voltage, current, and power injection at the slack bus. Also, let $\mathbf{v} := (\mathbf{v}_1^\mathsf{T}, \dots, \mathbf{v}_N^\mathsf{T})^\mathsf{T}$, $\mathbf{i} := (\mathbf{i}_1^\mathsf{T}, \dots, \mathbf{i}_N^\mathsf{T})^\mathsf{T}$, $\mathbf{i}^\Delta := ((\mathbf{i}_1^\Delta)^\mathsf{T}, \dots, (\mathbf{i}_N^\Delta)^\mathsf{T})^\mathsf{T}$, $\mathbf{s}^Y := ((\mathbf{s}_1^Y)^\mathsf{T}, \dots, (\mathbf{s}_N^Y)^\mathsf{T})^\mathsf{T}$, and $\mathbf{s}^\Delta := ((\mathbf{s}_1^\Delta)^\mathsf{T}, \dots, (\mathbf{s}_N^\Delta)^\mathsf{T})^\mathsf{T}$ be the vectors in $\mathbb{C}^{3N}$ collecting the relevant quantities of the PQ buses. The load-flow problem is then defined as solving for $\mathbf{v}$ (and $\mathbf{i}^\Delta, \mathbf{s}_0$) in the following set of equations, where $\mathbf{s}^Y$, $\mathbf{s}^\Delta$, and $\mathbf{v}_0$ are given:

$$\mathsf{diag}\left(\mathbf{H}^\mathsf{T}\overline{\mathbf{i}^\Delta}\right)\mathbf{v} + \mathbf{s}^Y = \mathsf{diag}(\mathbf{v})\bar{\mathbf{i}}, \tag{1a}$$

$$\mathbf{s}^\Delta = \mathsf{diag}\left(\mathbf{H}\mathbf{v}\right)\overline{\mathbf{i}^\Delta}, \tag{1b}$$

$$\mathbf{i} = \mathbf{Y}_{L0}\mathbf{v}_0 + \mathbf{Y}_{LL}\mathbf{v}, \tag{1c}$$

$$\mathbf{s}_0 = \mathsf{diag}(\mathbf{v}_0)\left(\overline{\mathbf{Y}}_{00}\overline{\mathbf{v}}_0 + \overline{\mathbf{Y}}_{0L}\overline{\mathbf{v}}\right). \tag{1d}$$

Here, $\mathbf{Y}_{00} \in \mathbb{C}^{3\times 3}, \mathbf{Y}_{L0} \in \mathbb{C}^{3N\times 3}, \mathbf{Y}_{0L} \in \mathbb{C}^{3\times 3N}$, and $\mathbf{Y}_{LL} \in \mathbb{C}^{3N\times 3N}$ are the submatrices of the three-phase admittance matrix

$$\mathbf{Y} := \begin{bmatrix} \mathbf{Y}_{00} & \mathbf{Y}_{0L} \\ \mathbf{Y}_{L0} & \mathbf{Y}_{LL} \end{bmatrix} \in \mathbb{C}^{3(N+1)\times 3(N+1)}; \tag{2}$$

and $\mathbf{H}$ is a block-diagonal matrix defined by

$$\mathbf{H} := \begin{bmatrix} \mathbf{\Gamma} & & \\ & \ddots & \\ & & \mathbf{\Gamma} \end{bmatrix}, \quad \mathbf{\Gamma} := \begin{bmatrix} 1 & -1 & 0 \\ 0 & 1 & -1 \\ -1 & 0 & 1 \end{bmatrix}. \tag{3}$$

The solution $\mathbf{v}$ to the set (1) can be found from the following fixed-point equation [11]:

$$\begin{aligned} \mathbf{v} &= \mathbf{G}_{\mathbf{s}^Y\mathbf{s}^\Delta}(\mathbf{v}) \\ &:= \mathbf{w} + \mathbf{Y}_{LL}^{-1}\left(\mathsf{diag}(\overline{\mathbf{v}})^{-1}\bar{\mathbf{s}}^Y + \mathbf{H}^\mathsf{T}\mathsf{diag}\left(\mathbf{H}\overline{\mathbf{v}}\right)^{-1}\bar{\mathbf{s}}^\Delta\right), \end{aligned} \tag{4}$$

where[1] $\mathbf{w} := -\mathbf{Y}_{LL}^{-1}\mathbf{Y}_{L0}\mathbf{v}_0$ is the zero-load voltage. In [11], explicit conditions for the existence and uniqueness of solutions to (4) were given. In the next section, we examine linear models that are based on (4).

Remark 1. Observe that (4) can be straightforwardly utilized in cases when a network features a mix of three-phase, two-phase, and single-phase buses. In particular, in that case, the vectors $\mathbf{v}$, $\mathbf{s}^Y$, and $\mathbf{w}$ collect their corresponding electrical quantities only for existing phases; the vector $\mathbf{s}^\Delta$ collects the existing phase-to-phase injections; and the matrix $\mathbf{H}$ contains rows that correspond to the existing phase-to-phase connections. For example, if a certain bus has only a single ab connection, it will contain only a row with $(1, -1, 0)$ for that bus. In this case, $\mathbf{H}$ is $N^\Delta \times N^{phases}$ matrix, where N^Δ is the total number of phase-to-phase connections, and N^{phases} is the total number of phases in all the buses.

Remark 2. For exposition simplicity, the proposed method is outlined for the case of a constant-power load model. This is also motivated by recent optimization and control frameworks for distribution systems, wherein distributed energy resources as well as noncontrollable assets are (approximately) modeled

[1]The matrix $\mathbf{Y}_{LL}$ is typically invertible; see [7], [15] for details.

as constant-PQ units [1], [3]–[5], [8]. However, the results in this paper can be naturally extended to a more general ZIP load model using a technique similar to [16].

III. Linear Power-Flow Models

In this section, we propose a method to linearize the power-flow equations (1). The method is based on a single iteration of the fixed-point equation (4).

Let $\mathbf{p}^Y := \Re\{\mathbf{s}^Y\}$, $\mathbf{q}^Y := \Im\{\mathbf{s}^Y\}$, $\mathbf{p}^\Delta := \Re\{\mathbf{s}^\Delta\}$, $\mathbf{q}^\Delta := \Im\{\mathbf{s}^\Delta\}$, $\mathbf{x}^Y := ((\mathbf{p}^Y)^\mathsf{T}, (\mathbf{q}^Y)^\mathsf{T})^\mathsf{T}$, and $\mathbf{x}^\Delta := ((\mathbf{p}^\Delta)^\mathsf{T}, (\mathbf{q}^\Delta)^\mathsf{T})^\mathsf{T}$ collect the active and reactive power injections. Also, let $|\mathbf{v}|$ collect the voltage magnitudes. Our goal is to derive linear approximations to (1) in the form

$$\widetilde{\mathbf{v}} = \mathbf{M}^Y\mathbf{x}^Y + \mathbf{M}^\Delta\mathbf{x}^\Delta + \mathbf{a}, \tag{5a}$$

$$|\widetilde{\mathbf{v}}| = \mathbf{K}^Y\mathbf{x}^Y + \mathbf{K}^\Delta\mathbf{x}^\Delta + \mathbf{b}, \tag{5b}$$

$$\widetilde{\mathbf{s}}_0 = \mathbf{G}^Y\mathbf{x}^Y + \mathbf{G}^\Delta\mathbf{x}^\Delta + \mathbf{c}. \tag{5c}$$

Based on (5a), we are also interested in the approximate linear relationship between line currents and net injected powers as:

$$\widetilde{\mathbf{i}}_{ij} = \mathbf{J}_{ij}^Y\mathbf{x}^Y + \mathbf{J}_{ij}^\Delta\mathbf{x}^\Delta + \mathbf{c}_{ij}, \tag{6}$$

where $\mathbf{i}_{ij} := (i_{ij}^a, i_{ij}^b, i_{ij}^c)^\top \in \mathbb{C}^3$, and i_{ij}^ϕ is the current entering phase ϕ of line (i,j) at bus i.

Note that the motivation for the explicit linear model for the voltage magnitudes (5b) stems from a typical constraint of the form $\mathbf{v}_{\min} \le |\widetilde{\mathbf{v}}| \le \mathbf{v}_{\max}$, which is nonconvex in $\mathbf{x}^Y$ and $\mathbf{x}^\Delta$, even if $\widetilde{\mathbf{v}}$ itself is linear in these variables. Also, observe that the explicit linear model for the current magnitudes is *not* required because the typical constraint used in power-network control and optimization is of the form $|\widetilde{\mathbf{i}}_{ij}| \le \mathbf{i}_{\max}$, which is convex whenever $\widetilde{\mathbf{i}}_{ij}$ is linear in $\mathbf{x}^Y$ and $\mathbf{x}^\Delta$. Finally, the motivation for the linear model for the power flow at the substation (5c) stems from aggregation and virtual power plant applications.

A. Voltage Phasors

Let $\widehat{\mathbf{v}}, \widehat{\mathbf{s}}^Y, \widehat{\mathbf{s}}^\Delta$ be a given solution for the fixed-point equation (4). Consider the first iteration of the fixed-point method initialized at $\widehat{\mathbf{v}}$:

$$\widetilde{\mathbf{v}} = \mathbf{w} + \mathbf{Y}_{LL}^{-1}\left(\mathsf{diag}(\overline{\widehat{\mathbf{v}}})^{-1}\overline{\mathbf{s}^Y} + \mathbf{H}^\mathsf{T}\mathsf{diag}\left(\mathbf{H}\overline{\widehat{\mathbf{v}}}\right)^{-1}\overline{\mathbf{s}^\Delta}\right), \tag{7}$$

which gives an *explicit* linear model (5a) provided by

$$\mathbf{M}^Y := \left(\mathbf{Y}_{LL}^{-1}\mathsf{diag}(\overline{\widehat{\mathbf{v}}})^{-1}, -\jmath\mathbf{Y}_{LL}^{-1}\mathsf{diag}(\overline{\widehat{\mathbf{v}}})^{-1}\right)$$

$$\mathbf{M}^\Delta := \left(\mathbf{Y}_{LL}^{-1}\mathbf{H}^\mathsf{T}\mathsf{diag}\left(\mathbf{H}\overline{\widehat{\mathbf{v}}}\right)^{-1}, -\jmath\mathbf{Y}_{LL}^{-1}\mathbf{H}^\mathsf{T}\mathsf{diag}\left(\mathbf{H}\overline{\widehat{\mathbf{v}}}\right)^{-1}\right)$$

and $\mathbf{a} = \mathbf{w}$.

This linear model has several important advantages. First, it is computationally efficient compared to, e.g., the first-order Taylor method [6], [11]. Second, the coefficients $(\mathbf{M}^Y)_{ij}$ depend only on the voltage of bus j for all i and similarly for $\mathbf{M}^\Delta$. Thus, this model naturally lends itself to distributed control and OPF methods. We refer to this second property as *distributability* and illustrate its utility in Section V-A.

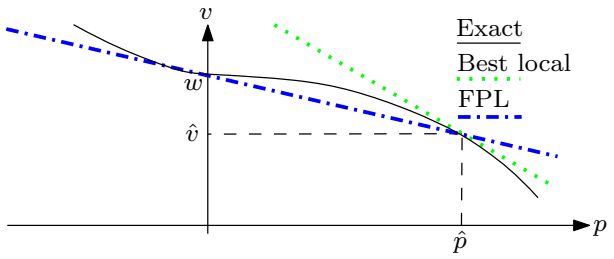

Fig. 2: Illustration of the difference between the tangent-plane and fixed-point linearization (FPL) methods. By definition, the tangent-plane method is the best local approximator.

Finally, if global behavior is of interest, it can also provide a better approximation than local methods; see, e.g., Figure 2, theoretical and numerical results in [11], and numerical experiments in Section IV of the present paper. In particular, Figure 2 shows that the fixed-point linearization method is an *interpolation* between two load-flow solutions: $(\mathbf{w}, \mathbf{0})$ and $(\widehat{\mathbf{v}}, \widehat{\mathbf{s}})$. This is in contrast to standard linearization methods that typically yield the tangent plane of the power-flow manifold at a given linearization point (e.g., the first-order Taylor method in [11] or the methodology of [8]).

B. Voltage Magnitudes

A straightforward approach to obtain a linear model for the voltage magnitudes $|\mathbf{v}|$ in (5b) is to leverage the following derivation rule:

$$\frac{\partial|f(x)|}{\partial x} = \frac{1}{|f(x)|}\Re\left\{\overline{f(x)}\frac{\partial f(x)}{\partial x}\right\}. \tag{8}$$

It then follows that matrices $\mathbf{K}^Y$ and $\mathbf{K}^\Delta$ are given by:

$$\mathbf{K}^Y := \frac{\partial|\mathbf{v}|}{\partial\mathbf{x}^Y} = \mathsf{diag}(|\widehat{\mathbf{v}}|)^{-1}\Re\left\{\mathsf{diag}(\overline{\widehat{\mathbf{v}}})\mathbf{M}^Y\right\}, \tag{9a}$$

$$\mathbf{K}^\Delta := \frac{\partial|\mathbf{v}|}{\partial\mathbf{x}^\Delta} = \mathsf{diag}(|\widehat{\mathbf{v}}|)^{-1}\Re\left\{\mathsf{diag}(\overline{\widehat{\mathbf{v}}})\mathbf{M}^\Delta\right\}, \tag{9b}$$

$$\mathbf{b} := |\widehat{\mathbf{v}}| - \mathbf{K}^Y\widehat{\mathbf{x}}^Y - \mathbf{K}^\Delta\widehat{\mathbf{x}}^\Delta. \tag{9c}$$

However, observe that model (9) lacks the important distributability property of model (7). Particularly, the coefficients $(\mathbf{K}^Y)_{ij}$ depend on both the voltage at bus i and j, and similarly for $\mathbf{K}^\Delta$.

We therefore develop a linear approximation of the voltage magnitudes based on the assumption that *the voltage drops are much smaller than the nominal voltage*, similar to, e.g., [17]. To this end, let $\mathbf{W} = \mathsf{diag}(\mathbf{w})$. By taking the absolute value on both sides of (7), we obtain

$$\begin{aligned}|\widetilde{\mathbf{v}}| &= \left|\mathbf{w} + \mathbf{M}^Y\mathbf{x}^Y + \mathbf{M}^\Delta\mathbf{x}^\Delta\right| \\ &= |\mathbf{W}|\left|\mathbf{1} + \mathbf{W}^{-1}(\mathbf{M}^Y\mathbf{x}^Y + \mathbf{M}^\Delta\mathbf{x}^\Delta)\right| \\ &\approx |\mathbf{W}|\left(\mathbf{1} + \Re\left\{\mathbf{W}^{-1}(\mathbf{M}^Y\mathbf{x}^Y + \mathbf{M}^\Delta\mathbf{x}^\Delta)\right\}\right)\end{aligned} \tag{10}$$

where the approximate equality follows under the assumption that

$$\left\|\mathbf{W}^{-1}(\mathbf{M}^Y\mathbf{x}^Y + \mathbf{M}^\Delta\mathbf{x}^\Delta)\right\|_\infty \ll 1. \tag{11}$$

Based on (10), we obtain a linear model (5a) with

$$\mathbf{K}^Y := |\mathbf{W}| \Re\left\{\mathbf{W}^{-1}\mathbf{M}^Y\right\}, \tag{12a}$$
$$\mathbf{K}^\Delta := |\mathbf{W}| \Re\left\{\mathbf{W}^{-1}\mathbf{M}^\Delta\right\}, \tag{12b}$$
$$\mathbf{b} := |\mathbf{w}|. \tag{12c}$$

Note that, compared to (9), the model (12) is distributable because the coefficients $(\mathbf{K}^Y)_{ij}$ depend only on the voltage at node j for all i, and similarly for $\mathbf{K}^\Delta$. In Section IV, we assess numerically the validity of assumption (11) and the accuracy of the proposed approximation.

C. Power Flow at the Substation

We obtain (5c) by directly utilizing (5a) and (1d), so that

$$\mathbf{G}^Y = \mathsf{diag}(\mathbf{v}_0)\overline{\mathbf{Y}}_{0L}\overline{\mathbf{M}}^Y, \; \mathbf{G}^\Delta = \mathsf{diag}(\mathbf{v}_0)\overline{\mathbf{Y}}_{0L}\overline{\mathbf{M}}^\Delta, \tag{13a}$$
$$\mathbf{c} = \mathsf{diag}(\mathbf{v}_0)\left(\overline{\mathbf{Y}}_{00}\overline{\mathbf{v}}_0 + \overline{\mathbf{Y}}_{0L}\overline{\mathbf{a}}\right). \tag{13b}$$

Note that this model is distributable as well.

D. Line Currents

Let $\mathbf{Z}_{ij} \in \mathbb{C}^{3\times 3}$ denote the phase impedance matrix[2] of distribution line (i,j), and $\mathbf{Y}_{ij}^{(s)} \in \mathbb{C}^{3\times 3}$ denote the shunt admittance matrix of the same line [12]. Per bus i, define the matrix $\mathbf{E}_i := [\mathbf{0}_{3\times 3(i-1)}, \mathbf{I}_3, \mathbf{0}_{3\times 3(N-i)}]$, and notice that the voltage vector $\mathbf{v}_i = (v_i^a, v_i^b, v_i^c)^\top$ can be rewritten as $\mathbf{v}_i = \mathbf{E}_i\mathbf{v}$. With these definitions in place, the line currents $\mathbf{i}_{ij}$ can be related to the voltage vector $\mathbf{v}$ as follows:

$$\begin{aligned}\mathbf{i}_{ij} &= \mathbf{Y}_{ij}^{(s)}\mathbf{v}_i + \mathbf{Z}_{ij}^{-1}(\mathbf{v}_i - \mathbf{v}_j)\\ &= \left(\mathbf{Y}_{ij}^{(s)} + \mathbf{Z}_{ij}^{-1}\right)\mathbf{E}_i\mathbf{v} - \mathbf{Z}_{ij}^{-1}\mathbf{E}_j\mathbf{v}\\ &= \left[\left(\mathbf{Y}_{ij}^{(s)} + \mathbf{Z}_{ij}^{-1}\right)\mathbf{E}_i - \mathbf{Z}_{ij}^{-1}\mathbf{E}_j\right]\mathbf{v}. \end{aligned} \tag{14}$$

Using (5a) in (14), it follows that a linear approximation $\mathbf{i}_{ij} = \mathbf{J}_{ij}^Y\mathbf{x}^Y + \mathbf{J}_{ij}^\Delta\mathbf{x}^\Delta + \mathbf{c}_{ij}$ can be readily obtained by setting the model parameters $\mathbf{J}_{ij}^Y$, $\mathbf{J}_{ij}^\Delta$, and $\mathbf{c}_{ij}$ to:

$$\mathbf{J}_{ij}^Y := \left[\left(\mathbf{Y}_{ij}^{(s)} + \mathbf{Z}_{ij}^{-1}\right)\mathbf{E}_i - \mathbf{Z}_{ij}^{-1}\mathbf{E}_j\right]\mathbf{M}^Y \tag{15a}$$
$$\mathbf{J}_{ij}^\Delta := \left[\left(\mathbf{Y}_{ij}^{(s)} + \mathbf{Z}_{ij}^{-1}\right)\mathbf{E}_i - \mathbf{Z}_{ij}^{-1}\mathbf{E}_j\right]\mathbf{M}^\Delta \tag{15b}$$
$$\mathbf{c}_{ij} := \left[\left(\mathbf{Y}_{ij}^{(s)} + \mathbf{Z}_{ij}^{-1}\right)\mathbf{E}_i - \mathbf{Z}_{ij}^{-1}\mathbf{E}_j\right]\mathbf{w}. \tag{15c}$$

IV. Numerical Evaluation

In this section, we assess numerically the approximation error of the proposed linear models; for theoretical analysis, refer to [11]. Two benchmark networks are used to perform the experiments: the IEEE 13-node feeder [18] and the Electric Power Research Institute (EPRI) J1 feeder [14]. The former is characterized by having short, relatively highly loaded overhead and underground lines, shunt capacitors, an in-line transformer, and unbalanced mixed wye and delta loading. The latter is a large network in the northeastern United States with approximately 2000 nodes and 800 connections at the primary side.

[2]The phase impedance matrix is typically invertible; see [12].

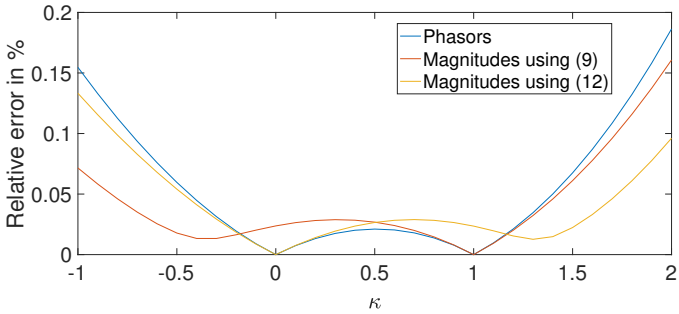

Fig. 3: Approximation error for voltages for the 13-bus feeder.

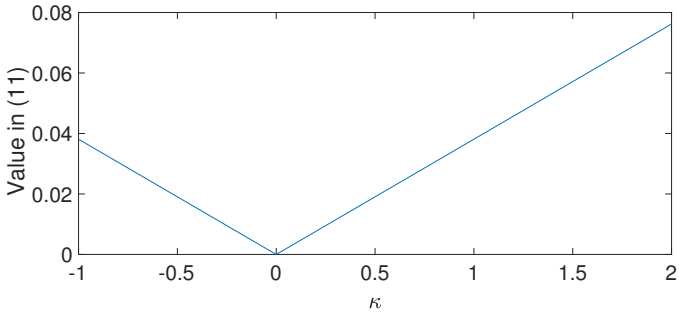

Fig. 4: Verification of the "small votlage drop" assumption (11) for the 13-bus feeder.

To assess the performance for different generation/loading conditions, we perform a *continuation analysis*: given a reference vector of power injections $\mathbf{s}^{\text{ref}}$, we evaluate the approximation error of the linear models by setting $\mathbf{s} = \kappa\mathbf{s}^{\text{ref}}$, for $\kappa \in \mathbb{R}$. All the computations were performed in the per unit (pu) system of the corresponding feeder.

A. IEEE 13-Bus Feeder

Similar to prior works [1], [3]–[5], [8], we first translate all constant-current and constant-impedance sources in the IEEE data set into constant-power sources. Denote this reference power injection vector by $\mathbf{s}^{\text{ref}}$. Figure 3 shows the results of the continuation analysis for the relative errors for the voltage phasors and voltage magnitudes using $\kappa \in [-1, 2]$. The relative error for the voltage vectors $\mathbf{v}$ and $\widetilde{\mathbf{v}}$ is defined by $\|\mathbf{v} - \widetilde{\mathbf{v}}\|_2/\|\mathbf{v}\|_2$, and similarly for the magnitudes. As shown, linear models behave very well with relative errors less than 0.2%. Moreover, the methods provide for a good global approximation. This corroborates the intuitive illustration in Figure 2. Also, Figure 4 confirms that assumption (11) holds for the considered range of power setpoints.

In Figure 5, we show the results of the continuation analysis for the power flow at the substation in terms of the normalized error $\|\mathbf{s}_0 - \widetilde{\mathbf{s}}_0\|_2/S_{\max}$, where $S_{\max}$ is the maximum apparent power observed during this experiment. Also here, the approximation is good with errors less than 1.5%. Finally, Figure 6 shows the results of the continuation analysis for the current phasor of a line that connects buses 692 and 675 of the feeder. This line was chosen because it is an underground line with a non-negligible shunt admittance. The utilized metric

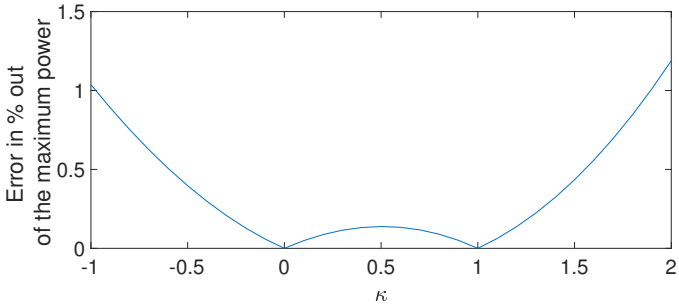

Fig. 5: Approximation error for power at the substation for the 13-bus feeder.

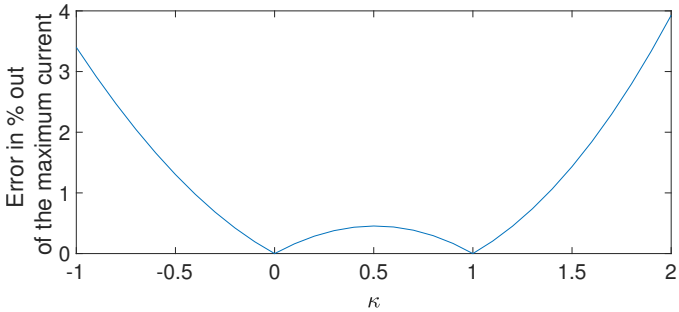

Fig. 6: Approximation error for the current phasor of line 692-675 of the 13-bus feeder.

is the normalized error $\|\mathbf{i}_{ij} - \widetilde{\mathbf{i}}_{ij}\|_2 / I_{\max}$, where $I_{\max}$ is the maximum current magnitude observed during this experiment. The obtained errors are less than 4%, confirming that our approach also provides good global approximation for the line currents. The errors for the other lines are on a similar scale, and the corresponding results are omitted due to space limitation.

B. EPRI J1 Feeder

Although the original feeder contains both delta and wye connections, the available data from [14] contains the equivalent wye injections for every bus. Using this injection vector as $\mathbf{s}^{\text{ref}}$, the continuation analysis for the voltages, voltage magnitudes, power flow at the substation, and line currents was performed using $\kappa \in [-1, 2]$. Figure 7 shows the relative errors for the voltage phasors and voltage magnitudes. It can be seen that the errors are less than 0.6%, illustrating that the proposed linear model performs well also for large distribution networks. The results for the power flow at the substation and line currents are on a scale that is similar to those for the 13-bus feeder, and they are omitted here because of space constraints.

V. Application Examples

In this section, we consider several applications in the context of real-time control.

A. Volt/VAR/Watt Control

Consider the design of the network-cognizant distributed Volt/VAR/Watt real-time controllers (or *voltage droop controllers*) similar to [9], [10]. In particular, the controllers react proportionally to the changes in voltage magnitude in real time. For brevity, let $\mathbf{x} := ((\mathbf{x}^Y)^\mathsf{T}, (\mathbf{x}^\Delta)^\mathsf{T})^\mathsf{T}$ and $\boldsymbol{\rho} := |\widetilde{\mathbf{v}}|$. Consider a given reference solution $(\overline{\boldsymbol{\rho}}, \overline{\mathbf{x}})$ to the linear model (10). Let $k = 1, 2, \ldots$ denote the time-step index, and let the voltage magnitudes at time step k be expressed as

$$\boldsymbol{\rho}(k) = \mathbf{K}(\mathbf{x}(k) + \boldsymbol{\Delta}\mathbf{x}(k)) + \mathbf{b}, \tag{16}$$

where $\mathbf{K} = (\mathbf{K}^Y, \mathbf{K}^\Delta) \in \mathbb{R}^{3N \times 12N}$, $\mathbf{x}(k) \in \mathbb{R}^{12N}$ is the vector of the power-setpoints throughout the feeder at time step k, and $\boldsymbol{\Delta}\mathbf{x}(k) \in \mathbb{R}^{12N}$ is the vector of the active and reactive power adjustments of the Volt/VAR/Watt controllers given by

$$\boldsymbol{\Delta}\mathbf{x}(k) = \mathbf{G}\boldsymbol{\Delta}\boldsymbol{\rho}(k-1). \tag{17}$$

In (17), $\boldsymbol{\Delta}\boldsymbol{\rho}(k-1) := \boldsymbol{\rho}(k-1) - \overline{\boldsymbol{\rho}}$ is the voltage deviation from the reference value; and $\mathbf{G}$ is the $12N \times 3N$ real matrix composed of $\mathbf{G} = (\mathbf{G}_p^Y, \mathbf{G}_q^Y, \mathbf{G}_p^\Delta, \mathbf{G}_q^\Delta)^\mathsf{T}$, where the matrices $\mathbf{G}_p^Y, \mathbf{G}_q^Y, \mathbf{G}_p^\Delta, \mathbf{G}_q^\Delta$ are diagonal $3N \times 3N$ matrices collecting the corresponding droop coefficient on their diagonals.

Using (16) and (17), the dynamical system for the voltage deviation vector $\boldsymbol{\Delta}\boldsymbol{\rho}(k)$ is given by

$$\boldsymbol{\Delta}\boldsymbol{\rho}(k) = \mathbf{K}\boldsymbol{\Delta}\mathbf{x}_{nc}(k) + \mathbf{K}\mathbf{G}\boldsymbol{\Delta}\boldsymbol{\rho}(k-1), \tag{18}$$

where $\boldsymbol{\Delta}\mathbf{x}_{nc}(k) := \mathbf{x}(k) - \overline{\mathbf{x}}$ is the uncontrollable deviation from the reference power setpoint. As in [10], consider that a forecast $\boldsymbol{\mu}$ is available for $\boldsymbol{\Delta}\mathbf{x}_{nc}(k)$, and let the modified dynamical system be:

$$\mathbf{e}(k) = \mathbf{K}\boldsymbol{\mu} + \mathbf{K}\mathbf{G}\mathbf{e}(k-1), \tag{19}$$

which converges to

$$\mathbf{e}^* = (\mathbf{I} - \mathbf{K}\mathbf{G})^{-1}\mathbf{K}\boldsymbol{\mu} \approx (\mathbf{I} + \mathbf{K}\mathbf{G})\mathbf{K}\boldsymbol{\mu} \tag{20}$$

under the condition that the spectral radius of $\mathbf{K}\mathbf{G}$ is less than 1; the approximate equality follows by using the first two terms of the Neuman series of a matrix [19] (see [10] for further details and stability analysis). We note that $\mathbf{e}^*$ is an approximation of the asymptotic voltage deviation from the reference value.

We next propose a network-cognizant distributed method to minimize (20). The idea is to to minimize the voltage deviation by bringing $\mathbf{K}\mathbf{G}$ as close as possible to $-\mathbf{I}$ while

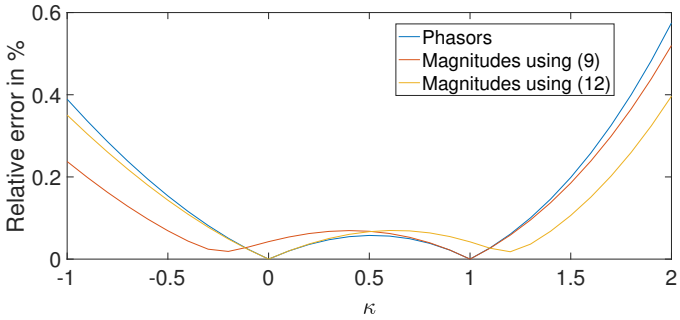

Fig. 7: Approximation error for the voltages for the EPRI J1 feeder.

keeping the spectral radius of $\mathbf{KG}$ below 1 for stability. The key to this is the fact that the columns of $\mathbf{KG}$ depend only on the voltage of the corresponding bus of the network and on the droop coefficients of this bus. In particular, let $\boldsymbol{\alpha}_j$ denote that j-th column of $\mathbf{KG}$. Because the linear model is distributable, $\boldsymbol{\alpha}_j$ depends only on the voltage at bus j and on the droop coefficients of bus j; let us denote this dependency as $\boldsymbol{\alpha}_j(\widehat{\mathbf{v}}_j, \mathbf{g}_j)$, where the vector $\mathbf{g}_j \in \mathbb{R}^{12}$ collects the droop coefficients of bus j.

Moreover, the stability condition can also be ensured in a distributed way by upper bounding the spectral radius with the ℓ_1-induced matrix norm. Specifically, we can ensure

$$\|\mathbf{KG}\|_1 = \max_j \|\boldsymbol{\alpha}_j(\widehat{\mathbf{v}}_j, \mathbf{g}_j)\|_1 < 1 \tag{21}$$

by ensuring $\|\boldsymbol{\alpha}_j(\widehat{\mathbf{v}}_j, \mathbf{g}_j)\|_1 < 1$ for every j in a distributed fashion.

To summarize, the following distributed algorithm is proposed:

(i) At the beginning of the process, send to all the devices the network model in the form of the matrices $\mathbf{Y}_{LL}^{-1}$ and $\mathbf{H}$.

(ii) On a slow time-scale (e.g., every 5-15 minutes or when there are significant voltage changes), solve the following optimization problem at every device j:

$$\inf_{\mathbf{g}_j} \quad \|\boldsymbol{\alpha}_j(\widehat{\mathbf{v}}_j, \mathbf{g}_j) + \mathbf{e}_j\|_2^2 \tag{22a}$$

$$\text{subject to}$$

$$\|\boldsymbol{\alpha}_j(\widehat{\mathbf{v}}_j, \mathbf{g}_j)\|_1 < 1, \tag{22b}$$

where $\mathbf{e}_j$ is the j-th column of the identity matrix. Note that to make (22) practically useful, the strict inequality constraint (22b) needs to be replaced with the inequality constraint by introducing stability margin parameter; see [10] for details. As $\boldsymbol{\alpha}_j(\widehat{\mathbf{v}}_j, \mathbf{g}_j)$ is a linear function of $\mathbf{g}_j$, the problem (22) is a convex optimization problem that can be solved efficiently.

(iii) In real time, adjust the active and reactive power setpoints according to (17) using the droop coefficients computed in step (ii).

Note that the algorithm proposed in this section is a simple example of how to design a network-cognizant, distributed real-time control algorithm using the distributable linear power-flow model. A thorough treatment of this and other control algorithms, including theoretical analysis and numerical experiments, is a subject of ongoing work.

B. Extension of Existing Methods

Approximate linear models that relate voltages and powers at the point of common coupling with net nodal power injections were utilized in [4], [5] to develop real-time and distributed OPF solvers for distribution systems with optimality and input-to-state stability guarantees. The models (12) and (13) can be leveraged to broaden the applicability of the algorithms proposed in [4], [5] to multiphase settings with a variety of electrical connections.

Similarly, the local control methods proposed in [9], [10] for voltage-regulation purposes can be re-engineered based on (12) to control renewable sources of energy with line-to-line connections.

VI. Conclusion

This paper outlined linear power-flow models for general multiphase distribution systems. The models are computationally efficient and are useful in decentralized and distributed OPF and real-time control settings due to their distributability. The performance of the models was numerically evaluated on two test feeders, and application examples were presented.

References

[1] S. H. Low, "Convex relaxation of optimal power flow – part I: Formulations and equivalence," *IEEE Transactions on Control of Network Systems*, vol. 1, no. 1, pp. 15–27, March 2014.

[2] H. Zhu and G. B. Giannakis, "Power system nonlinear state estimation using distributed semidefinite programming," *IEEE Journal of Selected Topics in Signal Processing*, vol. 8, no. 6, pp. 1039–1050, Dec 2014.

[3] S. Guggilam, E. Dall'Anese, Y. Chen, S. Dhople, and G. B. Giannakis, "Scalable optimization methods for distribution networks with high PV integration," *IEEE Transactions on Smart Grid*, 2015, submitted.

[4] A. Bernstein, L. E. Reyes Chamorro, J.-Y. Le Boudec, and M. Paolone, "A composable method for real-time control of active distribution networks with explicit power set points. part I: Framework," *Electric Power Systems Research*, vol. 125, no. August, pp. 254–264, 2015.

[5] E. Dall'Anese and A. Simonetto, "Optimal power flow pursuit," *IEEE Transactions on Smart Grid*, 2016, to appear.

[6] K. Christakou, J.-Y. Le Boudec, M. Paolone, and D.-C. Tomozei, "Efficient Computation of Sensitivity Coefficients of Node Voltages and Line Currents in Unbalanced Radial Electrical Distribution Networks," *IEEE Transactions on Smart Grid*, vol. 4, no. 2, pp. 741–750, 2013.

[7] S. Dhople, S. Guggilam, and Y. Chen, "Linear approximations to ac power flow in rectangular coordinates," *Allerton Conference on Communication, Control, and Computing , in Press*, 2015.

[8] S. Bolognani and F. Dörfler, "Fast power system analysis via implicit linearization of the power flow manifold," *Allerton Conference on Communication, Control, and Computing , in Press*, 2015.

[9] K. Baker, A. Bernstein, C. Zhao, and E. Dall'Anese, "Network-cognizant design of decentralized volt/var controllers," in *The Eighth Conference on Innovative Smart Grid Technologies (ISGT 2017)*, 2017.

[10] K. Baker, A. Bernstein, E. Dall'Anese, and C. Zhao, "Network-cognizant voltage droop control for distribution grids," 2017, [Online] Available at: http://arxiv.org/abs/1702.02969.

[11] A. Bernstein, C. Wang, E. Dall'Anese, J.-Y. Le Boudec, and C. Zhao, "Load-flow in multiphase distribution networks: Existence, uniqueness, and linear models," 2017, [Online] Available at: http://arxiv.org/abs/1702.03310.

[12] W. H. Kersting, *Distribution System Modeling and Analysis*. 2nd ed., Boca Raton, FL: CRC Press, 2007.

[13] ——, "A comprehensive distribution test feeder," in *IEEE PES Transmission and Distribution Conference and Exposition*, April 2010, pp. 1–4.

[14] Electric Power Research Institute (EPRI). Distributed PV Monitoring and Feeder Analysis. [Online]. Available: http://dpv.epri.com/feeder_models.html

[15] C. Wang, A. Bernstein, J.-Y. Le Boudec, and M. Paolone, "Existence and uniqueness of load-flow solutions in three-phase distribution networks," *IEEE Transactions on Power Systems*, vol. PP, no. 99, pp. 1–1, 2016.

[16] M. Bazrafshan and N. Gatsis, "Convergence of the Z-bus method for three-phase distribution load-flow with ZIP loads," 2016, [Online] Available at: https://arxiv.org/abs/1605.08511.

[17] S. Bolognani and S. Zampieri, "On the existence and linear approximation of the power flow solution in power distribution networks," *IEEE Trans. on Power Systems*, 2015.

[18] W. H. Kersting, "Radial distribution test feeders," in *IEEE Power Engineering Society Winter Meeting*, vol. 2, 2001, pp. 908–912.

[19] R. A. Horn and C. R. Johnson, *Matrix analysis*. Cambridge University Press, 1990.